SAND83-0025

A COMPARISON OF FREE COMPONENT MODE SYNTHESIS TECHNIQUES USING MSC/NASTRAN

D. R. Martinez and D. L. Gregory
Sandia National Laboratories*
Albuquerque, New Mexico 87185

ABSTRACT

MSC/NASTRAN was used to compare three techniques of component mode synthesis (CMS) using free modes. A free-free beam model was analyzed by the three methods and compared to the finite element results for the entire beam. The three CMS techniques use different combinations of assumed displacement vectors. Two of the techniques are available as standard options within MSC/NASTRAN. The third utilizes residual terms and is ideally suited to using results from an experimental data base to describe a portion of the model. For this technique, we have studied the effects of including residual terms only in the stiffness matrix or in both the mass and stiffness matrices, as well as neglecting the off-diagonal residual terms. Significant divergence of low frequency system modes was obtained when using one technique while excellent and identical convergence was obtained using the other two. Results are given for modal frequency convergence.

---

*This work was sponsored by the U. S. Department of Energy under Contract No. DE-AC04-76-DP00789.

INTRODUCTION

Component mode synthesis (CMS) is a technique of dynamic substructuring and reduction for large finite element models. It may be classified as a Ritz transformation technique, in which an approximate mathematical description of the total system model is developed from individual models of the components or subsystem parts.* The solution of the original model is approximated by a summation of assumed displacement shapes or Ritz vectors. The coefficients of the Ritz vectors are the generalized coordinates used to describe a reduced order model. In the CMS technique, the assumed vectors include both static and dynamic displacement shapes. The structure is first divided into subsystems containing both interior and interface degrees-of-freedom (DOF). The subsystems are also referred to as components, substructures, or superelements. The Ritz vectors are selected in a predetermined fashion, based on the static and dynamic characteristics of the individual subsystems. A modal analysis of each subsystem is then performed using either free or fixed interface DOF, and a truncated set of the resulting eigenvectors are used as the dynamic displacement shapes. Typically, the eigenvectors associated with the lowest component modes are retained to form the truncated set.

To achieve accurate dynamic response using CMS techniques, the dynamic displacement shapes must be supplemented with static displacement shapes [2]. These are typically determined from a Guyan reduction of the interior DOF of the subsystem stiffness matrix, or from residual

---

* For more background material and a definition of terms, see Craig [1]. (Numbers in square brackets [ ] refer to references listed at the end of the paper.)

flexibility effects resulting from the use of a truncated set of eigenvectors. Various types of static shapes may be obtained from the stiffness matrix and modal characteristics of the subsystem. The boundary conditions used in calculating the dynamic mode shapes of the subsystem will determine which static displacement shapes should be used.

The static and dynamic displacement shapes are used to define a reduction transformation. Then, the mass, stiffness, and damping matrices for each subsystem are reduced to to an approximate, lower order model. Both physical and generalized coordinates may be used to describe the subsystem equations. The equations for all the subsystems are then combined to form the system equations by invoking interface displacement and force compatibility. If desired, the response of the interior DOF for each subsystem may also be obtained. Because generalized coordinates are used to describe the subsystems, the final system model generally has significantly fewer DOF than the original model of the entire system. The objective is to maintain a specified level of accuracy in the dynamic analysis while using the lower order model for computational efficiency.

CMS techniques may also be used as a tool to couple experimental and analytical models. The modern vibration test lab can now provide an experimental modal description of a structure or subsystem. This data base consists of the modal frequencies, mode shapes, modal mass, and modal damping. In addition, a quantity referred to as residual flexibility may be obtained with some of the curve fitting algorithms which are currently available in commercial modal analysis software [3]. This experimental data base contains the information neccessary to formulate the reduced subsystem matrices required for use in the synthesis of the system model.

Because of these advances in experimental modal analysis and testing, there has been a great interest in utilizing the measured modal data base for further analysis [4]. Instead of using the measured modes only to verify an existing finite element (FE) model, attempts are being made to directly utilize the measured data base in a combined experimental/analytical model. These techniques have been used in the aerospace and automotive industries for several years [5,6,7]. In the aerospace industry, fixed interface modes have been most often measured. Then, a detailed FE model of the subsystem which was tested is used to orthogonalize the measured modes [8] and to obtain the static modes and static contribution to the reduced mass and stiffness matrices for the subsystem. The static portion of the reduced model may also be obtained without the use of the FE model if the interface modal forces are measured during the vibration test [9].

In some applications, free interface elastic modes are measured. For some structures, these are easier to obtain experimentally than fixed interface modes. As in the case with fixed interface modes, the static portion of the reduced model may be determined from a finite element model or from test. To experimentally determine the static effects, either mass loading of the interface must be included when measuring the modes, or the residual flexibility properties of the test item must be measured [10,11,12]. Using current commercially available modal analysis software, it is possible to estimate residual flexibility in addition to the elastic modal properties [3]. For those applications where it is desired to obtain the subsystem description entirely from test, the use of free elastic modes and residual flexibility properties is a very attractive approach.

In this study, MSC/NASTRAN was used to evaluate a CMS technique using free interface dynamic modes, and static modes determined from the residual flexibility. This technique was compared to the two CMS options currently in MSC/NASTRAN which use free interface modes. A free-free beam model was analyzed by the three techniques and compared to the finite element results for the entire beam. A brief summary of the development of the equations used for the residual flexibility CMS technique is given, followed by results for modal frequency convergence.
For completeness, results from the standard fixed interface CMS technique which is available in MSC/NASTRAN are also included.

DESCRIPTION OF THE THREE COMPONENT MODE SYNTHESIS TECHNIQUES

There are two basic combinations of static and dynamic displacement shapes that are most useful when developing a combined experimental/analytical model. Fixed interface elastic mode shapes are typically supplemented with static displacement shapes determined from the standard Guyan reduction of interior DOF to the interface DOF [1]. These static shapes are referred to as constraint modes. They are the columns of the Guyan reduction transformation matrix. Free interface dynamic mode shapes are supplemented with a variety of static displacement shapes. A very logical and accurate technique [1] uses static shapes which are determined from the residual flexibility associated with a truncated set of elastic modes. These are referred to as residual attachment modes. They are certain columns of the residual flexibility matrix. Alternatively, free elastic modes may be augmented with constraint modes; however, for

subsystems with rigid body motion, additional static vectors called inertia relief (IR) shapes must also be used [13].

The three CMS techniques which were compared are characterized by their use of different displacement shapes. Method 1 uses free interface elastic modes and constraint modes. This is the standard free CMS formulation currently in MSC/NASTRAN, Version 62. Method 2 uses free interface elastic modes and constraint modes, but adds inertia relief shapes as additional static modes. This is the optional formulation currently in Version 62. Method 3 uses free interface dynamic modes plus residual attachment modes. Method 3 is not currently available in MSC/NASTRAN and was programmed into the normal modes rigid format, Solution 63, using standard DMAP matrix modules [14]. For Method 3, we have studied the effects of including residual terms only in the stiffness matrix or in both the mass and stiffness matrices, as well as neglecting the off-diagonal residual terms. The development of Methods 1 and 2 is given by Herting [13]. Method 3 is a Ritz transformation technique, developed following the approach used by Craig [15,16]; however, the final form of the equations are given by an alternative expression which explicitly retains the interface DOF as physical coordinates in the reduced system model. This feature simplifies the coupling of subsystems and, in general, permits the reduced dynamic characteristics of each subsystem to be obtained with either fixed or free interface DOF.

Other CMS techniques have employed the use of residual terms. The free mode residual technique developed by MacNeal [17], and improved by Rubin [18], is obtained using a different approach than Craig, but it can be shown that they arrive at similar results. For the eigenvalue problem, the basic technique of Method 3 reduces to the same form as

Rubin. (The fixed interface CMS technique is described in [19,20].)

The motivation for comparing the three CMS techniques was to to evaluate the acceptability of the residual flexibility technique for combined experimental/analytical modeling. For this technique, if the static contributions to the subsystem matrices are to be obtained from test, measurements of rotational frequency response functions and rotational residual flexibilities are neccessary. If the static contributions are to be determined by a FE model of the subsystem, only the elastic and rigid body modes must be measured. If a FE model for the subsystem is used, the inertia relief shape technique is also a candidate for use in combined experimental/analytical modeling. In this case, only elastic modes must be measured, and either free or fixed modes are acceptable.

RESIDUAL FLEXIBILITY CMS TECHNIQUE USING FREE MODES

A development of the residual flexibility CMS technique which was programmed into MSC/NASTRAN is included in Appendix I. The original motivation was to evaluate a CMS technique for forced response calculations which was consistent with that used to obtain combined experimental/analytical models using free modes. In particular, the effect of residual mass as well as the treatment of loads on interior DOF were of concern. In the general development, provision is made to include static displacement shapes for interior DOF where applied forces exist. Only the final form of the equations used for the eigenvalue analysis are given in this section.

The total transformation of the subsystem matrices is divided into two steps. The first step is the Ritz transformation which utlizes the free interface dynamic modes and residual attachment static modes. For unrestrained subsystems, rigid body modes must also be used, and the residual attachment modes must be calculated using inertia relief loading (see Craig [1]). The results of this first transformation are the reduced subsystem matrices expressed entirely in terms of generalized coordinates. When expressed in this form, the terms in the reduced subsystem matrices retain physical and intuitive interpretation. Also, the modal truncation effects are more easily understood. The second transformation replaces the generalized coordinates which are associated with the residual attachment modes, with the physical coordinates associated with the interface DOF. When expressed in this alternative formulation, the terms in the reduced subsystem matrices lose physical interpretation; however, this form greatly simplifies coupling of the subsystem equations to obtain the system equations.

The final form of the equations used for the eigenvalue problem are now summarized. All terms used in the equations in this section are described in detail in Appendix I. The subsystem equations, including the applied force terms are also given there. The original equation describing the subsystem in terms of physical coordinates is

$$M \ddot{\underline{x}} + K \underline{x} = \underline{F} \qquad (1)$$

Because the applied forces are not considered for the eigenvalue problem, the transformation used to approximate the subsystem displacement, $\underline{x}$, simplifies to

$$\underline{x} = \Phi_k \underline{q}_k + G_B \underline{q}_B = T_1 \underline{q} \qquad (2)$$

where $\underline{q}_k$ are the generalized coordinates associated with the kept dynamic component modes and $\underline{q}_B$ are the generalized coordinates associated with the residual attachment modes. Rigid body modes are contained in the $\underline{q}_k$ coordinates. The transformed subsystem equations become

$$M^R \ddot{\underline{q}} + K^R \underline{q} = \underline{F}^R \qquad (3)$$

As shown in Appendix I, the K^R and M^R matrices may be partitioned according to the $\underline{q}_k$ and $\underline{q}_B$ coordinates as follows,

$$K^R = \begin{bmatrix} \Omega_k^2 & 0 \\ 0 & G_{BB} \end{bmatrix} \qquad M^R = \begin{bmatrix} I_k & 0 \\ 0 & H_{BB} \end{bmatrix} \qquad (4)$$

Note that when expressed in this form, the dynamic and static portions of the reduced subsystem stiffness and mass matrices are uncoupled.

The alternate formulation for the subsystem equations is obtained by using a second transformation. This transformation replaces the generalized coordinates which are associated with the residual attachment modes, $\underline{q}_B$, with the physical coordinates associated with the interface DOF, $\underline{x}_B$. The partitioned stiffness and mass matrices become

$$K_2^R = \begin{bmatrix} \Omega_k^2 + \Phi_{kB}^T G_{BB}^{-1} \Phi_{kB} & -\Phi_{kB}^T G_{BB}^{-1} \\ \text{Sym} & G_{BB}^{-1} \end{bmatrix} \qquad (5a)$$

$$M_2^R = \begin{bmatrix} I_k + \Phi_{kB}^T J_{BB} \Phi_{kB} & -\Phi_{kB}^T J_{BB} \\ \text{Sym} & J_{BB} \end{bmatrix} \qquad (5b)$$

where $J_{BB} = G_{BB}^{-1} H_{BB} G_{BB}^{-1}$. See Appendix I for a definition of other terms.

The reduced system equations may now be obtained from direct matrix assembly using Equation (5). The only matrix inverse required is G_{BB}^{-1}, the partitioned residual flexibility matrix associated with the interface DOF. Note that because the interface DOF appear explicitly as physical coordinates in Equation (5), coupling of subsystems is straightforward; however, the interpretation of terms in the stiffness and mass matrices loses physical significance, which is apparent in Equation (4).

Equation (3) includes residual effects in both the stiffness and mass matrices and is a consistent Ritz transformation technique. An inconsistent but often used transformation neglects the residual mass effects [17]. This is equivalent to using a less accurate transformation to reduce M, defined by

$$\underline{x} = \Phi_k \underline{q}_k = [\Phi_k \; 0] \begin{Bmatrix} \underline{q}_k \\ \underline{q}_B \end{Bmatrix} = T_1' \, \underline{q} \qquad (6)$$

Note that if residual mass is neglected,

$$M^R = M_2^R = \begin{bmatrix} I_k & 0 \\ 0 & 0 \end{bmatrix} \qquad (7)$$

One of the variations of the residual flexibility CMS technique which was studied neglects the off-diagonal residual terms. The proper implementation of this technique

is not apparent when the subsystem equations are given in the form of Equation (5). The off-diagonal residual terms must be neglected in G_{BB} and H_{BB} as they appear in Equation (4). Then, the second transformation may be used to properly account for this effect in the form of the matrices as given in Equation (5).

A discussion of the calculations required to obtain the residual flexibility matrix is also given in Appendix I. First the total residual flexibility matrix must be calculated. Then, the flexibility matrix due to the kept elastic modes is subtracted out. The modes associated with the deleted elastic modes need not be calculated. For singular K matrices, a procedure which utilizes inertia relief loading must be used [1].

CASE STUDIES RESULTS

General Comments and Description of Model

The free-free beam that was modeled and used for the numerical study is described in Figure 1. This structure was also tested in a modal test lab. The beam was made of mild steel rectangular bar stock with a (0.5 x 1.0) inch cross section. To create low frequency torsion modes, four rectangular concentrated masses were placed in an asymmetric configuration along the length. Two identical beams were manufactured and one was physically cut into two subsystems. Modal frequencies and mode shapes were experimentally obtained for the complete beam as well as the two subsystems. Results of this experimental study showed excellent agreement between predicted and measured modes and will be documented in another paper.

The beam was modeled in MSC/NASTRAN [14] using lumped mass (CBAR) elements. The lumped mass moments of inertia of

the beam elements were also included at every grid point (GP) using CONM2 cards. The concentrated rectangular masses were assumed to be rigid and, for plotting purposes, were defined by four corner grid points. Their total mass and inertia was lumped at the center of each mass. The corner points were connected to the center point with RBE2 elements. The total number of DOF for the FE model of the entire beam was 318; 222 in the a-set, and 96 in the m-set (see [14] for the set notation definition).

Two different cases were used for dividing the model into subsystems, as shown in Figure 2. In both cases, the beam was divided into two subsystems or superelements, denoted SE10 and SE20. To avoid confusion with the term residual, for all cases, the reduced system models will be referred to as approximate models or reduced structure models rather than residual structure models, as is the standard MSC/NASTRAN nomenclature. The first case (denoted as one-point) consisted of a reduced structure model which contained only one physical grid point, GP-1. The second case (denoted as two-point) retained two GP's as physical DOF in the reduced structure. The one-point case corresponded to the beam and subsystems which were tested. The two-point case was neccessary because a numerical instability was encountered when applying CMS Methods 1 and 2 in the one-point case. Consequently, the two-point case was used when comparing Method 3 with Methods 1 and 2. The one-point case was used when comparing the various forms of Method 3. The total number of component modes for SE10 was 126 elastic and 6 rigid body. For the one-point case, the total number for SE20 was 90 elastic and 6 rigid body. The two-point case had only 84 elastic modes in SE 20.

The mass moments of inertia for each beam element were included to ensure there were always at least six interface

DOF with non-zero mass for each subsystem. The number of interface DOF determine the number of static modes which will be calculated and used in the transformation of each subsystem. It was found that if less than six non-zero mass DOF existed at the subsystem interfaces, eigenvalue convergence could not be obtained for the approximate models, even if all the elastic component modes were retained.

The modal frequencies and mode shapes for the FE model of the entire beam were obtained using the normal modes rigid format. This solution was used as the reference solution for the numerical study. The beam has four distinct types of modes, denoted softwise bending, stiffwise bending, torsion, and axial. The four types of modes must be examined separately to properly understand the effects of modal truncation. Also, when evaluating modal frequency convergence for the various techniques, care must be taken to ensure that corresponding modes are compared. Mismatching of some modes can easily occur due to truncation effects, as well as in areas of high modal density. As can be seen in the tables, if the modal frequencies for the approximate models are simply listed in numerical order, some of the modes switch order relative to the reference modes.

The proper matching of modes is accomplished through the use of a quantity called the mode shape correlation coefficient (MSCC), defined by Ibrahim [21]. The MSCC determines the correlation or "resemblance" between any two mode shapes. In addition, because the approximate mode shapes are compared to the mode shapes from the reference model, for this study, the MSCC provides a quantity that is

useful in determining the accuracy of the approximate mode shapes. The MSCC is defined as

$$MSCC = \frac{|\underline{\phi}_{app}^{T} \underline{\phi}_{ex}^{*}|^2}{|\underline{\phi}_{app}^{T} \underline{\phi}_{app}^{*}| \; |\underline{\phi}_{ex}^{T} \underline{\phi}_{ex}^{*}|} \qquad (8)$$

where $\underline{\phi}_{app}$ is the approximate mode shape, $\underline{\phi}_{ex}$ is the reference mode shape and '*' denotes complex conjugate. Although this quantity is a more forgiving measure of convergence than a direct percentage error, it is very useful for comparing the ammount of correlation or coherent information in the approximate vs. the reference mode shapes.

Two-Point Case Results

Figure 3 shows the modal frequency convergence of the various CMS techniques for the softwise bending modes. Figure 4 shows the results for the stiffwise bending modes. Percent errors, relative to the reference solution, are plotted as a function of mode number. The frequencies associated with each mode number are also shown. There were a total of 20 modes in the frequency range of interest, which was zero to 2000Hz. Because there were only three torsional modes and one axial mode in this frequency range, results are plotted only for the bending modes.

The curves are identified by a title, and by the total number of approximate system modes, as well as the number of kept elastic component modes from SE10 and SE20. For example, component modes to 2000Hz were retained for Method

2 (denoted as MSC/NASTRAN w/IR, 39 - 9/6). This consisted of nine elastic modes from SE10 and six from SE20, six inertia relief shapes from each superelement, and six constraint modes from each superelement corresponding to the six interface DOF. This results in 39 total system modes. Modes to 2000Hz were also retained for Method 1 (denoted MSC/NASTRAN w/o IR, 27 - 9/6) but, because Method 1 does not use the inertia relief shapes, there are 12 fewer DOF in the approximate system model. Consequently, results from a second calculation for Method 1 are also shown, in which component modes to 3500Hz were retained, yielding 39 total system modes.

Component modes to 2000Hz were also retained for the Method 3 results. Two versions of Method 3 are shown. The consistent version of Method 3, which includes both residual stiffness and mass, is denoted as the RKM technique. The inconsistent version, which neglects the effects of residual mass, is denoted as the RK technique. In each case, 39 total system modes were retained. This consisted of nine elastic modes from SE10 and six from SE20, six rigid body modes from each superelement, and six residual attachment modes from each superelement corresponding to the six interface DOF. For completeness, results from the fixed CMS technique in MSC/NASTRAN are also included in which component modes to 2300Hz were retained, yielding 39 total system modes.

These results show identical convergence for the RKM technique and Method 2. For these two techniques, excellent results are obtained up to the truncation frequency of the component modes. The RK technique and the fixed CMS technique give less accurate results than Method 2 and RKM; however, the errors are still very small. For the RK technique, there is an error of less than 1% for 16 of the

20 modes in the frequency range of interest. Further, 18 of the 20 modes have an error less than 2%. These figures also show the neccessity of including the inertia relief shapes when using free interface elastic modes and static constraint modes as the total transformation for an unrestrained subsystem. Large errors exist in many of the lowest modes for the non-inertia relief shape technique. Clearly, if rigid body component modes exist as in this example, the non-inertia relief option is not acceptable.

One-Point Case Results

Two studies were performed to evaluate the specific characteristics of Method 3 which would be useful for developing combined experimental/analytical models. The effects of neglecting residual mass and/or the off-diagonal residual terms were studied. Results are shown in Figure 5. Component modes were retained to 2000Hz and results are shown from both the RK and RKM techniques. Neglecting residual mass causes a noticeable increase in the errors; however, for the RK technique, there are still 17 of the 20 modes of interest that have an error less than 2%. Further, although there is a noticeable error introduced when neglecting the off-diagonal residual terms, it is not significant. For the diagonal RK 2000Hz case, there are 16 of the 20 modes of interest that have an error less than 2%. The residual mass terms have a significant effect on the modes near the truncation frequency but they do have an effect on the low frequency modes as well. The excellent convergence which was achieved, even when neglecting both the residual mass and the off-diagonal residual stiffness terms, has important experimental implications for the

combined experimental/analytical modeling work. The diagonal residual stiffness terms are the simplest to determine experimentally.

Results from a low frequency convergence study are shown in Figure 6. Component modes were retained to 500 and 200Hz, respectively, for both the RKM and RK techniques. (For comparison, the RK 2000Hz results are also plotted in Figure 6.) These results indicate that if the residual terms are used, acceptable results may be obtained even when retaining a very small number of elastic modes. Note that the 200Hz RKM case is more accurate than the 500Hz RK case. The 200Hz case also shows an important effect of including the residual terms. The third system mode, which is the first torsional mode, was predicted accurately with no torsional component modes retained from either subsystem. It is strictly the effect of the residual terms which accounts for the accuracy of this mode.

CONCLUSIONS

MSC/NASTRAN was used to compare three techniques of component mode synthesis (CMS) to a reference finite element model for a free-free beam. The residual flexibility and inertia relief shape techniques gave excellent and identical results for both modal frequency convergence and mode shape correlation. The non-inertia relief shape technique cannot be used for subsystems with rigid body modes without a significant loss of accuracy in the low frequency approximate system modes. For the residual flexibility technique, neglecting residual mass caused a small increase in the errors. Neglecting the off-diagonal residual terms

in either mass or stiffness also caused a small increase in the errors.

The residual flexibility technique is ideally suited for situations where a subsystem definition is to be obtained entirely from a modal test using free subsystem modes. If a finite element model of the subsystem is to be used to provide the static portion of the reduced subsystem matrices, only the elastic and rigid body modes must be experimentally determined. For this case, either free or fixed elastic modes may be used and the inertia relief technique is also suitable for obtaining the combined experimental/analytical model.

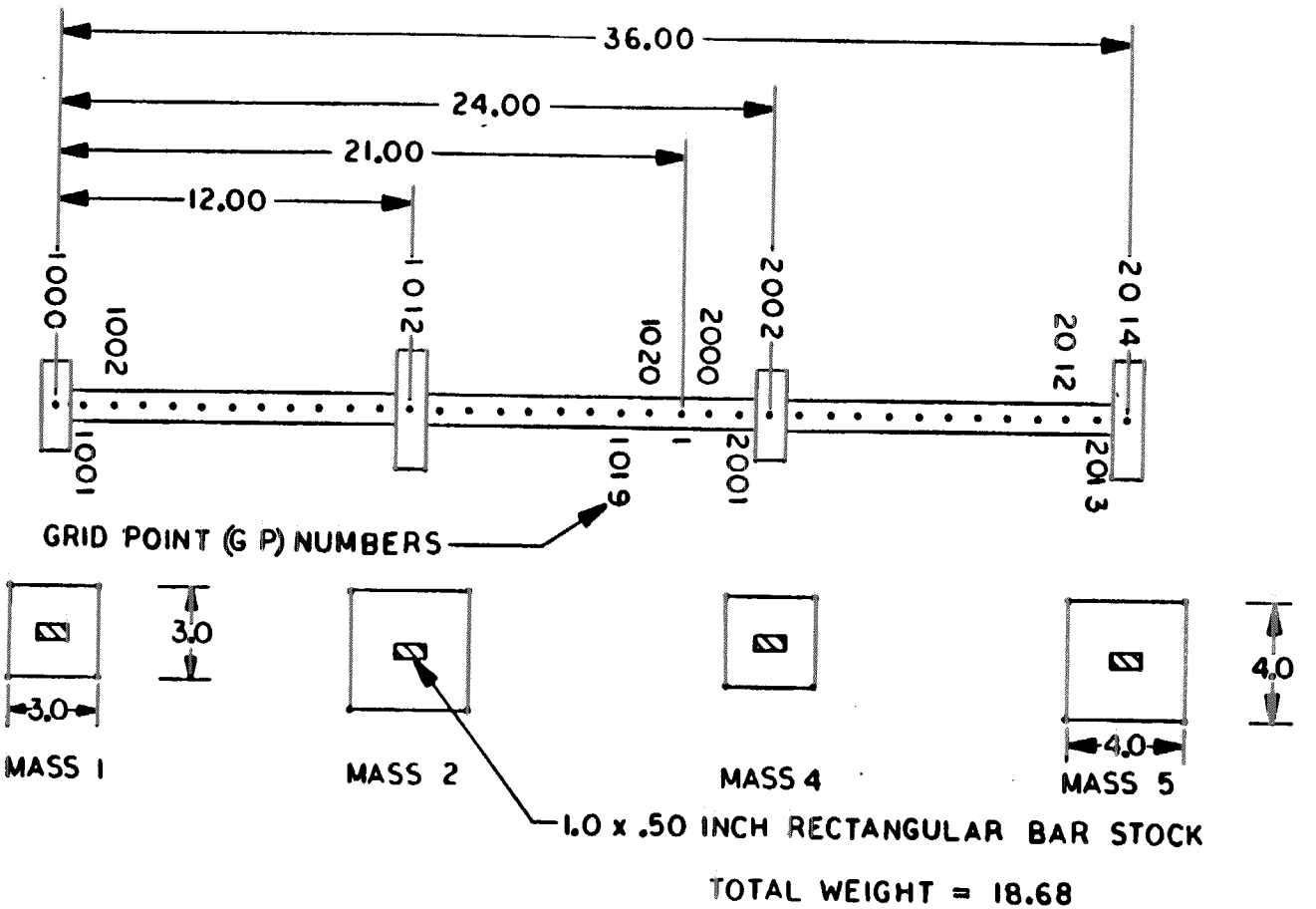

FIGURE 1. TEST BEAM DESCRIPTION

CASE 1 - TWO GRID POINTS IN RESIDUAL STRUCTURE

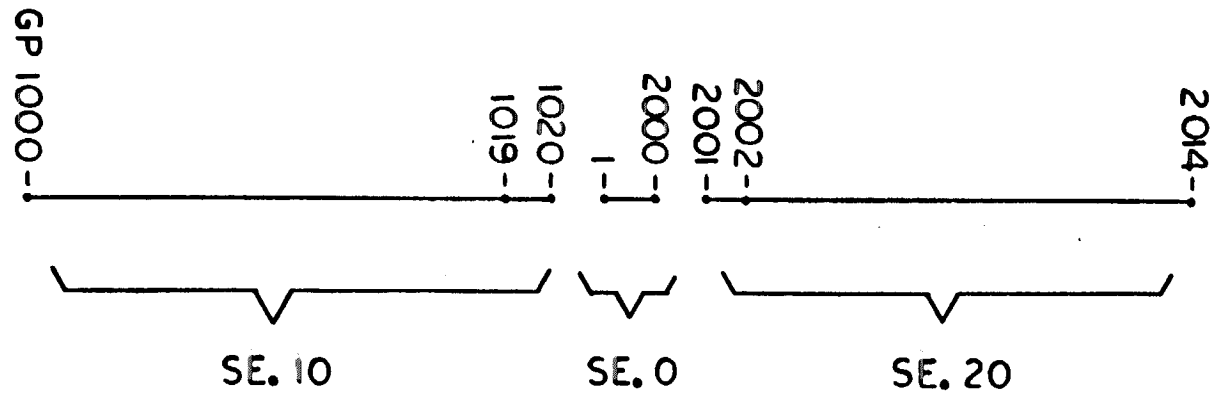

CASE 2 - ONE GRID POINT (GP) IN RESIDUAL STRUCTURE

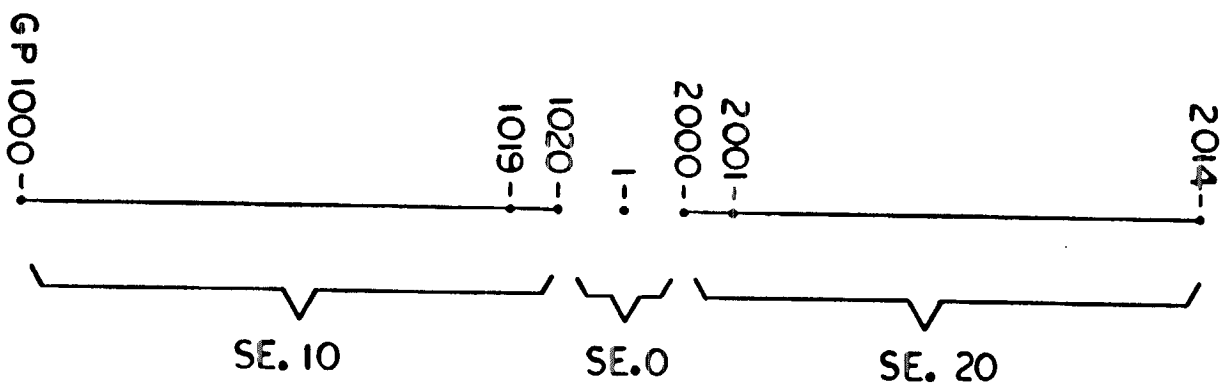

FIGURE 2. SUBSTRUCTURE DEFINITION

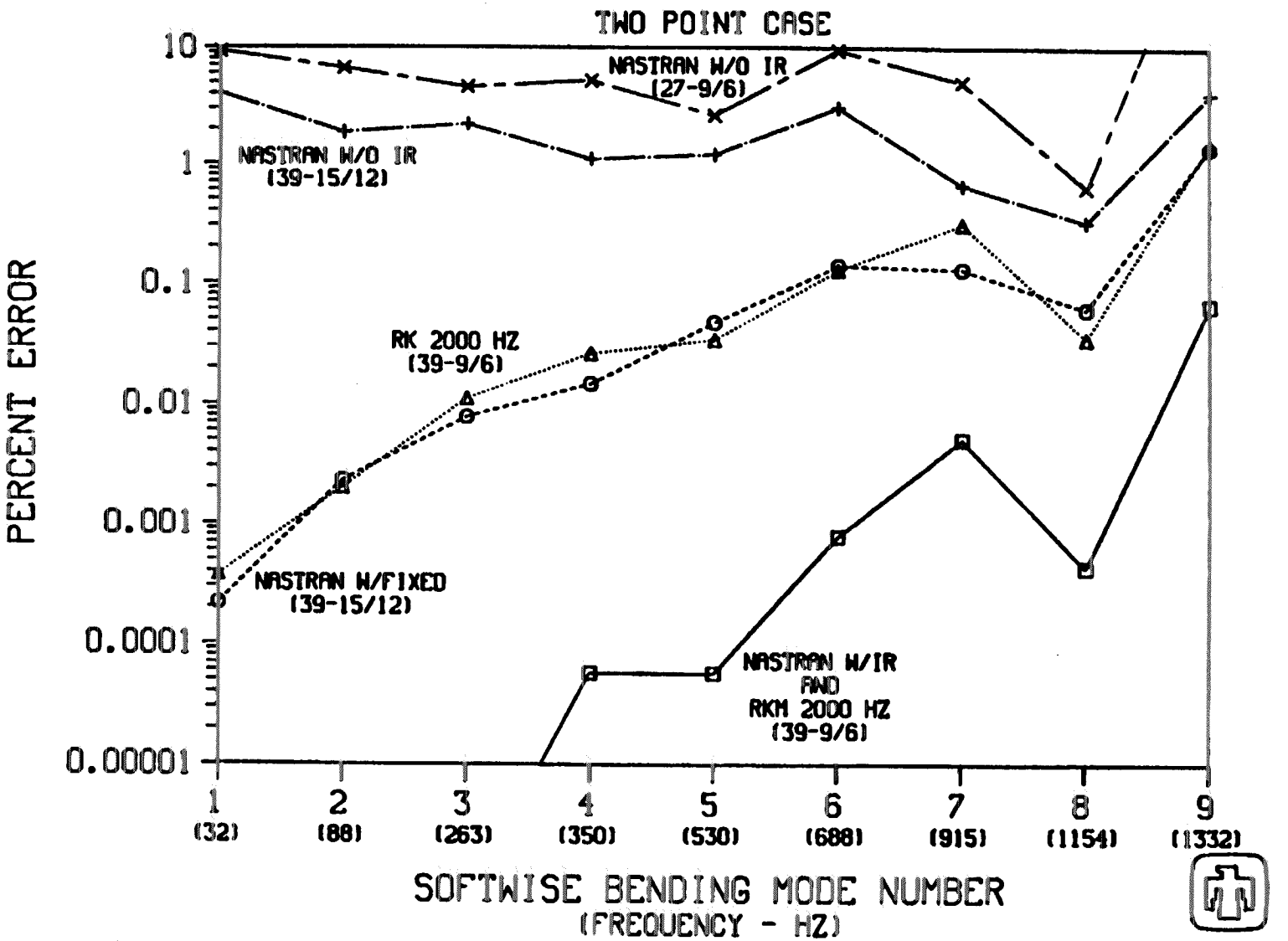

FIGURE 3. SOFTWISE BENDING MODAL FREQUENCY CONVERGENCE - TWO POINT CASE

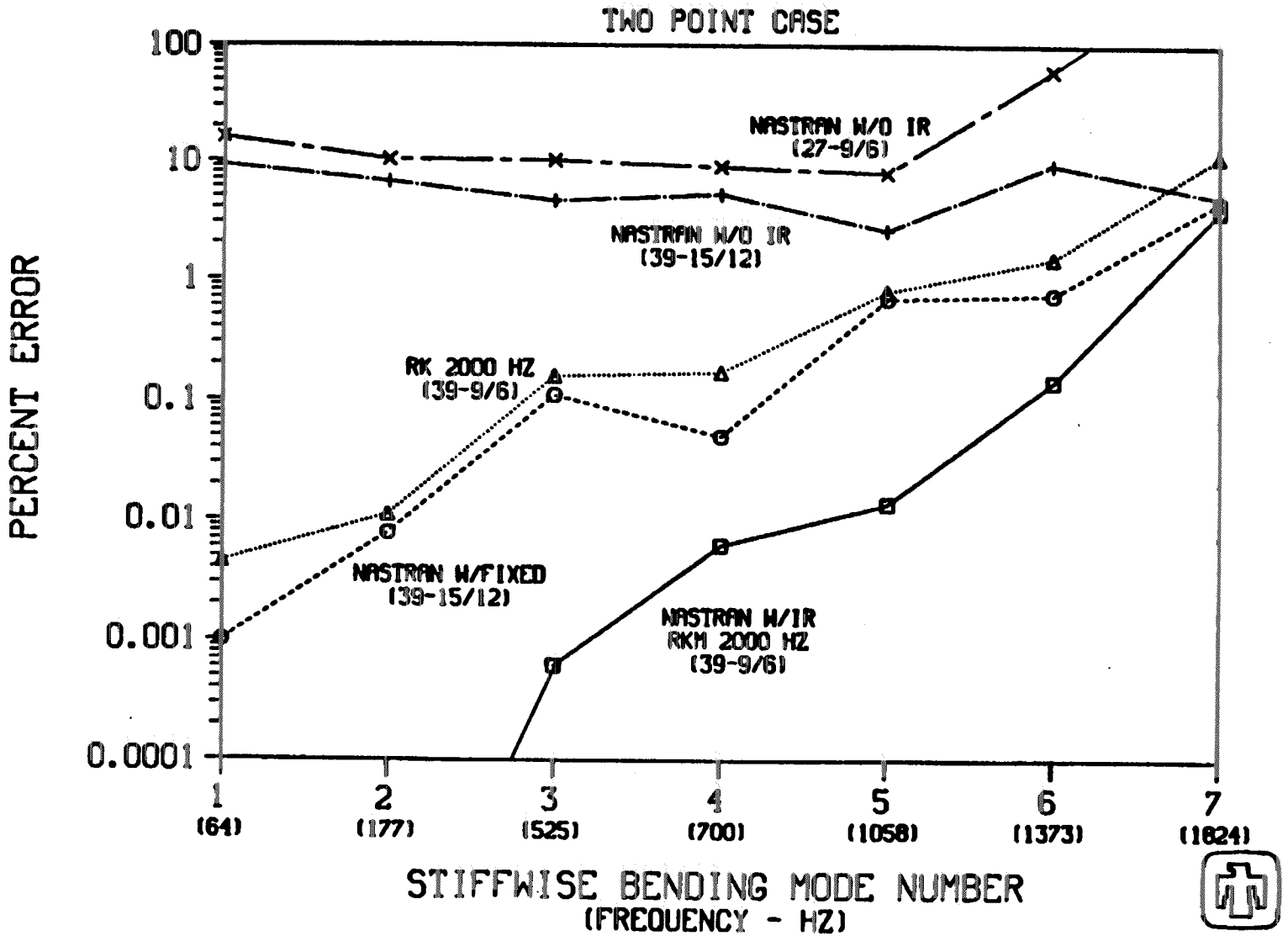

FIGURE 4. STIFFWISE BENDING MODAL FREQUENCY CONVERGENCE - TWO POINT CASE

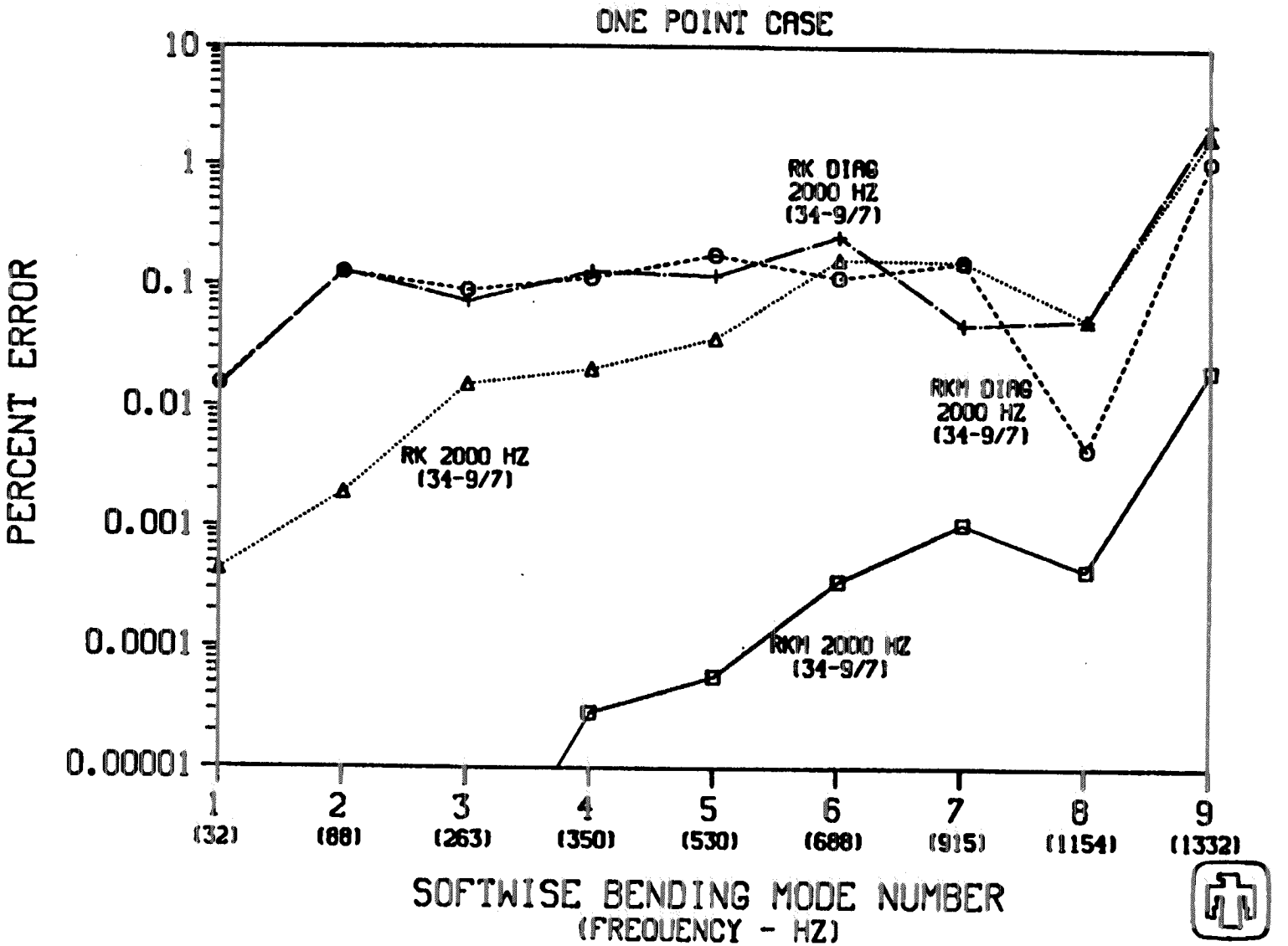

FIGURE 5. MODAL FREQUENCY CONVERGENCE - ONE POINT CASE

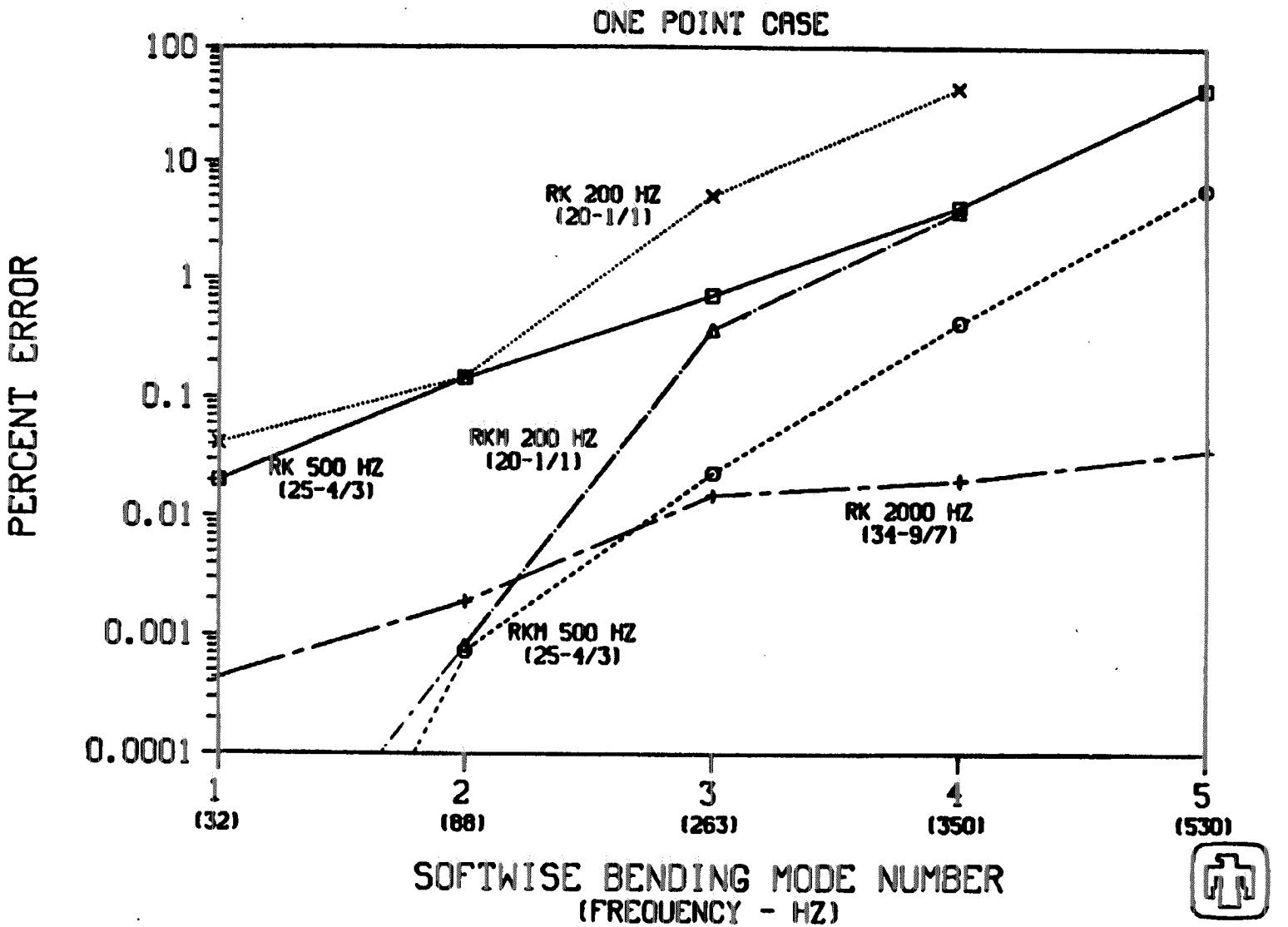

FIGURE 6. LOW FREQUENCY CONVERGENCE - ONE POINT CASE

REFERENCES

1. Craig, R.R., Jr., Structural Dynamics, An Introduction to Computer Methods, John Wiley and Sons, 1981.

2. Hintz, R. M., "Analytical Methods in Component Modal Synthesis", AIAA Journal, Vol. 13, No. 8, August 1975, pp. 1007-1016.

3. Modal-Plus Reference Manual, Version 6, The SDRC Corporation, Milford, Ohio, August, 1981.

4. First International Modal Analysis Conference, Proceedings, Orlando, Florida, sponsored by Union College, November, 1982

5. Klosterman, A. L. and McClelland, W. A., "Combining Experimental and Analytical Techniques for Dynamic System Analysis", Theory and Practice in Finite Element Structural Analysis, University of Tokyo Press, 1973, pp. 339-356.

6. Fleming, E. R., "Spacecraft Dynamic Loads, The Load Cycle Approach", Government/Industry Workshop on Payload/Loads Technology, Proceedings, NASA CP-2075, November, 1978, pp. 47-71.

7. Klosterman, A. L., On the Experimental Determination and Use of Modal Representations of Dynamic Characteristics, Ph.D. Dissertation, University of Cincinnati, 1971.

8. Targoff, W. P., "Orthogonality Check and Correction of Measured Modes", AIAA Journal, Vol 14, No. 2, February, 1976, pp. 164-167.

9. Dynamic Analysis of General Structures, User's Manual, The SDRC Corporation, Milford, Ohio.

10. Coppolino, R. N., "Employment of Residual Mode Effects in Vehicle/Payload Dynamic Loads Analysis", Government/Industry Workshop on Payload/Loads Technology, Proceedings, NASA CP-2075, November, 1978, pp. 323-346.

11. Benfield, W. A. and Hruda, R. F., "Vibration Analysis of Structures by Component Mode Substitution", AIAA Journal, Vol. 9, No. 7, July 1971, pp. 1255-1261.

12. Coppolino, R. N., private communications.

13. Herting, D. N., "A General Purpose, Multi-Stage, Component Modal Synthesis Method," MacNeal-Schwendler Corporation, to be published.

14. MSC/NASTRAN User's Manual, Version 62, 1982, C. W. McCormick, ed.

15. Craig, R.R., Jr. and Chang, C-J, "On the Use of Attachment Modes in Substructure Coupling for Dynamic Analysis," 18th Structural Dynamics and Materials Conference, San Diego, California, March 1977.

16. Chang, Ching-Jone, A General Procedure for Substructure Coupling in Dynamic Analysis, Ph.D Dissertation, Applied Mechanics Department, University of Texas at Austin, 1977.

17. MacNeal, R.H., "A Hybrid Method of Component Mode Synthesis," Journal of Computers and Structures, V.1, n.4, December 1971, pp. 581-601.

18. Rubin, S., "Improved Component-Mode Representation for Structural Dynamic Analysis," AIAA Journal, V.13 n.8, August 1975, pp. 995-1006.

19. Hurty, W.C., "Dynamic Analysis of Structural Systems Using Component Modes." AIAA Journal, V.3 n.4, April 1965, pp. 678-685.

20. Craig, R.R., Jr. and Bampton, M.C.C., "Coupling of Substructures for Dynamic Analysis," AIAA Journal, V.6, n.7, July 1968, pp.1313-1319.

21. Ibrahim, S.R. and Pappa, R.S., "Large Modal Survey Testing Using the Ibrahim Time Domain (ITD) Identification Technique," 22nd Structural Dynamics and Materials Conference, Atlanta, Georgia, April 1981.

22. Martinez, D.R. amd Miller, A.K., " Component Mode Synthesis for Forced Response Using Free Modes", to be published.

APPENDIX I

SUMMARY OF THE CMS TECHNIQUE USING RESIDUAL FLEXIBILITY AND FREE MODES

General Comments

A brief development of the residual flexibility CMS technique which was programmed into MSC/NASTRAN is given below. A more detailed derivation is presented in [22]. Provision is made to include static attachment modes for interior DOF where applied forces exist. The total transformation of the subsystem matrices is divided into two steps. The first is the Ritz transformation which utilizes the free interface dynamic modes and residual attachment static modes. For unrestrained subsystems, rigid body modes must also be used, and the residual attachment modes must be calculated using inertia relief loading (see Craig [1]). The results of this first transformation are subsystem matrices expressed entirely in terms of generalized coordinates. When expressed in this form, the terms in the reduced subsystem matrices retain physical and intuitive interpretation, and the effects of truncated modes are easily understood. The second transformation replaces the generalized coordinates which are associated with the interface static modes, with the physical coordinates associated with the interface DOF. Although the terms in the reduced subsystem matrices for this alternate definition lose physical interpretation, this form greatly simplifies the coupling of the subsystem equations to obtain the reduced system equations.

Subsystem Equations

The original equation describing the subsystem in terms of physical coordinates is

$$M\ddot{\underline{x}} + C\dot{\underline{x}} + K\underline{x} = \underline{F} \qquad (1)$$

where M,C, and K are the (N x N) mass, damping, and stiffness subsystem matrices; $\ddot{\underline{x}}$, $\dot{\underline{x}}$, and $\underline{x}$ are the acceleration, velocity, and displacement N-vectors; and $\underline{F}$ is the total subsystem forcing function. $\underline{x}$ and $\underline{F}$ are partitioned as follows;

$$\underline{x} = \begin{Bmatrix} \underline{x}_O \\ \underline{x}_I \\ \underline{x}_B \end{Bmatrix} \qquad \underline{F} = \begin{Bmatrix} \underline{0} \\ \underline{F}_I \\ \underline{F}_B + \underline{f}_B \end{Bmatrix} \qquad (2)$$

where $\underline{x}_B$ are the interface DOF, $\underline{x}_I$ are the interior DOF where external forces $\underline{F}_I$ are applied, $\underline{x}_O$ are the interior DOF without external applied forces, $\underline{F}_B$ are external applied forces on the $\underline{x}_B$ DOF, and $\underline{f}_B$ are the interface forces due to adjacent subsystems. (Note that K may be singular due to rigid body modes of the subsystem.) An eigenvalue analysis is performed on the undamped form of Equation (1). The eigenvectors are then used in the following transformation to approximate the subsystem displacement, $\underline{x}$,

$$\underline{x} = \Phi_k\underline{q}_k + G_I\underline{q}_I + G_B\underline{q}_B = T_1\underline{q} = [\Phi_k \; G_I \; G_B] \begin{Bmatrix} \underline{q}_k \\ \underline{q}_I \\ \underline{q}_B \end{Bmatrix} \qquad (3)$$

where Φ_k is an (N x n_k) matrix of kept component modes (elastic and rigid body), n_k is the number of kept modes, $\underline{q}_k$, $\underline{q}_I$, $\underline{q}_B$, and $\underline{q}$ are the generalized coordinate vectors,

G_I and G_B are partitions of the (N x N) residual flexibility matrix G, and T_1 is the total transformation matrix. G is defined as follows:

$$G = \sum_{i=n_k+1}^{N} \frac{\underline{\phi}_i \underline{\phi}_i^T}{\omega_i^2} \tag{4}$$

where $\underline{\phi}_i$ is the i-th deleted eigenvector, ω_i^2 is the i-th modal frequency, and the eigenvectors have been normalized to unity modal mass. G may be partitioned by columns, consistent with $\underline{x}$ and $\underline{F}$, as $G = [G_O \quad G_I \quad G_B]$. The full partitioning for G is

$$G = \begin{array}{c} \begin{array}{ccc} \overleftarrow{\quad n_O \quad} & \overleftarrow{\quad n_I \quad} & \overleftarrow{\quad n_b \quad} \end{array} \\ \begin{bmatrix} G_{OO} & G_{OI} & G_{OB} \\ G_{IO} & G_{II} & G_{IB} \\ G_{BO} & G_{BI} & G_{BB} \end{bmatrix} \end{array} \begin{array}{l} n_O \\ n_I \\ n_B \end{array} \tag{5}$$

where n_B are the number of interface DOF, n_I are number of interior DOF where external forces are applied, and n_O are the number of interior DOF without external applied forces. The transformation showing the full partitioning for T_1 is

$$\underline{x} = \begin{Bmatrix} \underline{x}_O \\ \underline{x}_I \\ \underline{x}_B \end{Bmatrix} = \begin{bmatrix} \Phi_{kO} & G_{OI} & G_{OB} \\ \Phi_{kI} & G_{II} & G_{IB} \\ \Phi_{kB} & G_{BI} & G_{BB} \end{bmatrix} \begin{Bmatrix} \underline{q}_k \\ \underline{q}_I \\ \underline{q}_B \end{Bmatrix} = T_1 \underline{q} \tag{6}$$

where the first column of T_1 is simply the partitioning of Φ_k consistent with $\underline{x}$. Because G may be calculated using only the deleted elastic modes, it can be shown [15,22] that Φ_k and G are orthogonal with respect to the M and K matrices, i.e.,

$$\Phi_k^T K G = 0 = \Phi_k^T M G \tag{7a}$$

Using the partitioning of G, we obtain

$$\begin{aligned} \Phi_k^T K G_I &= \Phi_k^T K G_B = 0 \\ \Phi_k^T M G_I &= \Phi_k^T M G_B = 0 \end{aligned} \tag{7b}$$

Also, it may be shown that [22]

$$G^T K G = G \tag{8a}$$

Expanding Equation (8a), we obtain

$$\begin{bmatrix} G_0^T K G_0 & G_0^T K G_I & G_0^T K G_B \\ & G_I^T K G_I & G_I^T K G_B \\ \text{Symmetric} & & G_B^T K G_B \end{bmatrix} = \begin{bmatrix} G_{00} & G_{0I} & G_{0B} \\ & G_{II} & G_{IB} \\ \text{Symmetric} & & G_{BB} \end{bmatrix} \tag{8b}$$

Applying T_1 to Equation (1), the transformed subsystem equations become

$$M^R \ddot{q} + C^R \dot{q} + K^R q = F^R \tag{9a}$$

where

$$M^R = T_1^T M T_1,\ C^R = T_1^T C T_1,\ K^R = T_1^T K T_1,\ \underline{F}^R = T_1^T \underline{F} \qquad (9b)$$

Expanding Equation (9b) and using Equations (7b,8b), we obtain

$$K^R = \begin{bmatrix} \Omega_k^2 & 0 & 0 \\ & G_{II} & G_{IB} \\ \text{Sym} & & G_{BB} \end{bmatrix} \qquad (10a)$$

$$M^R = \begin{bmatrix} I_k & 0 & 0 \\ & H_{II} & H_{IB} \\ \text{Sym} & & H_{BB} \end{bmatrix} \qquad (10b)$$

$$\underline{F}^R = \begin{bmatrix} \Phi_{kB}^T \\ G_{BI} \\ G_{BB} \end{bmatrix} (\underline{f}_B + \underline{F}_B) + \begin{bmatrix} \Phi_{kI}^T \\ G_{II} \\ G_{IB}^T \end{bmatrix} \underline{F}_I \qquad (10c)$$

where $\Omega_k^2 = \Phi_k^T K \Phi_k$, $I_k = \Phi_k^T M \Phi_k$, $H_{II} = G_I^T M G_I$, $H_{IB} = G_I^T M G_B$, $H_{BB} = G_B^T M G_B$, and C^R has a similar form to M^R. Ω_k^2 is a diagonal matrix of kept dynamic modes, and I_k is an identity matrix. Note that only certain partitions of the transformation matrix T_1 are needed to define the residual portion of K^R , i.e., the matrix products indicated in Equation (8) need not be performed. Equations (9,10) describe the reduced equations for the subsystem. Note that

residual effects due to the static displacement shapes defined by G_I and G_B are retained in the reduced mass (denoted residual mass), stiffness and damping matrices, as well as the reduced forcing function.

The above formulation is a consistent Ritz transformation technique. Residual effects are included in the stiffness, mass, and damping mass matrices. An inconsistent, but often used transformation, neglects the residual mass and damping effects [17]. If these terms are neglected, Equation (9a) may be partitioned and it may be shown that [22]

$$\underline{q}_I = \underline{F}_I \quad , \qquad \underline{q}_B = \underline{f}_B + \underline{F}_B \tag{11}$$

This is equivalent to using a less accurate transformation T_1' to reduce M and C where

$$\underline{x} = \Phi_k \underline{q}_k = [\Phi_k \; 0 \; 0] \begin{Bmatrix} \underline{q}_k \\ \underline{q}_I \\ \underline{q}_B \end{Bmatrix} = T_1' \; \underline{q} \tag{12}$$

Although this inconsistent formulation is less accurate, it is much easier to implement. Only the residual stiffness terms are needed, but these are defined by certain partitions of the residual flexibility matrix G. When the subsystem equations are expressed entirely in terms of generalized coordinates as in Equation (10), the residual mass terms are clearly seen.

To permit simple and general coupling between subsystems, it is convenient to obtain an alternate formulation for the subsystem equations. From the lower partition of Equation (6), it can be shown that

$$\underline{q}_B = -G_{BB}^{-1} \Phi_{kB} \underline{q}_k - G_{BB}^{-1} G_{BI} \underline{q}_I + G_{BB}^{-1} \underline{x}_B \tag{13}$$

Let $\underline{q}_2 = \left\{\underline{q}_k \; \underline{q}_I \; \underline{x}_B\right\}^T$. Then, a transformation T_2 can be introduced incorporating Equation (12) as follows,

$$\underline{q} = \begin{Bmatrix} \underline{q}_k \\ \underline{q}_I \\ \underline{q}_B \end{Bmatrix} = T_2 \, \underline{q}_2 = \begin{bmatrix} I & 0 & 0 \\ 0 & I & 0 \\ -G_{BB}^{-1} \, \Phi_{kB} & -G_{BB}^{-1} \, G_{BI} & G_{BB}^{-1} \end{bmatrix} \begin{Bmatrix} \underline{q}_x \\ \underline{q}_I \\ \underline{x}_B \end{Bmatrix} \tag{14}$$

The alternate subsystem equation becomes

$$M_2^R \, \ddot{\underline{q}} + C_2^R \, \dot{\underline{q}} + K_2^R \, \underline{q} = \underline{F}_2^R \tag{15}$$

where

$$K_2^R = \begin{bmatrix} \Omega_k^2 + \Phi_{kB}^T \, G_{BB}^{-1} \, \Phi_{kB} & 0 & -\Phi_{kB}^T \, G_{BB}^{-1} \\ & G_{II} - G_{BI}^T \, G_{BB}^{-1} \, G_{BI} & 0 \\ \text{Symmetric} & & G_{BB}^{-1} \end{bmatrix} \tag{16a}$$

$$M_2^R = \begin{bmatrix} I_k + \Phi_{kB}^T \, J_{BB} \, \Phi_{kB} & -\Phi_{kB}^T \, G_{BB}^{-1} \, J_{BI} & -\Phi_{kB}^T \, J_{BB} \\ & J_{II} - G_{BI}^T \, G_{BB}^{-1} \, J_{BI} & H_{IB} \, G_{BB}^{-1} - G_{BI}^T \, J_{BB} \\ \text{Symmetric} & & J_{BB} \end{bmatrix} \tag{16b}$$

$$\underline{F}_2^R = \begin{bmatrix} \Phi_{kI}^T - \Phi_{kB}^T G_{BB}^{-1} G_{IB}^T \\ G_{II} - G_{BI}^T G_{BB}^{-1} G_{IB}^T \\ G_{BB}^{-1} G_{IB}^T \end{bmatrix} \underline{F}_I + \begin{Bmatrix} 0 \\ 0 \\ \underline{f}_B + \underline{F}_B \end{Bmatrix} \qquad (16c)$$

and

$$\begin{aligned} J_{BB} &= G_{BB}^{-1} H_{BB} G_{BB}^{-1} \\ J_{BI} &= H_{BI} - H_{BB} G_{BB}^{-1} G_{BI} \\ J_{II} &= H_{II} - H_{IB} G_{BB}^{-1} G_{BI} \end{aligned} \qquad (16d)$$

C_2^R has a form similar to M_2^R .

The approximate system equations may now be obtained from direct matrix assembly using Equation (16). Because $\underline{x}_B$ appear explicitly as physical coordinates in the subsystem equations, coupling of subsystems is straightforward; however, the interpretation of terms in K_2^R , M_2^R , C_2^R , and $\underline{F}_2^R$ lose their physical significance which is apparent in Equation (10). The only matrix inverse required is G_{BB}^{-1} , the partitioned residual flexibility matrix associated with the interface DOF, $\underline{x}_B$.

The development given above applies to the general forced response problem. For the specific results reported in this study, we are interested only in the real eigenvalue problem. Then, C_2^R is neglected, $\underline{F}_I = \underline{F}_B \equiv \underline{0}$, and $\underline{q}_I$ is null. Equation (10) simplifies to

$$K^R = \begin{bmatrix} \Omega_k^2 & 0 \\ 0 & G_{BB} \end{bmatrix} \quad M^R = \begin{bmatrix} I_k & 0 \\ 0 & H_{BB} \end{bmatrix} \quad \underline{F}^R = \begin{bmatrix} \Phi_{kB}^T \\ G_{BB} \end{bmatrix} \underline{f}_B \qquad (17)$$

and Equation (16) simplifies to

$$K_2^R = \begin{bmatrix} \Omega_k^2 + \Phi_{kB}^T G_{BB}^{-1} \Phi_{kB} & -\Phi_{kB}^T G_{BB}^{-1} \\ \text{Sym} & G_{BB}^{-1} \end{bmatrix} \tag{18a}$$

$$M_2^R = \begin{bmatrix} I_k + \Phi_{kB}^T J_{BB} \Phi_{kB} & -\Phi_{kB}^T J_{BB} \\ \text{Sym} & J_{BB} \end{bmatrix} \tag{18b}$$

$$F_2^R = \begin{Bmatrix} \underline{0} \\ \underline{f}_B \end{Bmatrix} \tag{18c}$$

Note that if residual mass is neglected,

$$M^R = M_2^R = \begin{bmatrix} I_k & 0 \\ 0 & 0 \end{bmatrix} \tag{18d}$$

One of the variations of the residual flexibility CMS technique which was studied, neglects the off-diagonal residual terms. The proper implementation of this technique is not apparent when the subsystem equations are given in the form of Equation (16). The off-diagonal residual terms must be neglected in G_{BB} and H_{BB} as they appear in Equation (10). Then, the second transformation may be used to properly account for this effect in the form of the matrices as given in Equation (16).

Calculation of Residual Attachment Modes

The residual flexibility matrix may be obtained directly from Equation (4); however, all deleted elastic modes from n_k+1 to N are required. In this section, for clarity, we denote the residual flexibility as G^d. Alternatively, if the total elastic flexibility matrix, G^e, is obtained first, the flexibility due to the kept modes, G^k, may be subtracted out to obtain G^d, i.e.

$$G^d = G^e - G^k \tag{19}$$

It can be shown [1] that Equation (19) may be written in terms of the modes as

$$G^e = \Phi_e \Omega_e^{-2} \Phi_e^T = \Phi_{ke} \Omega_{ke}^{-2} \Phi_{ke}^T + \Phi_d \Omega_d^{-2} \Phi_d^T \tag{20}$$

where $\Phi_e = [\Phi_r \ \Phi_{ke} \ \Phi_d]$ is the total component eigenvector matrix, Φ_R are the rigid body modes, Φ_{ke} are the kept elastic modes, Φ_d are the deleted elastic modes, Ω_e^{-2} is the inverse of the diagonal matrix of all elastic modes, Ω_{ke}^{-2} is the inverse of the diagonal matrix of kept elastic modal frequencies, and Ω_d^{-2} is the inverse of the diagonal matrix of deleted elastic modal frequencies. For unrestrained subsystems the stiffness matrix is singular. In this case, the residual attachment modes must be calculated using inertia relief loading (see Craig [1]). This procedure is briefly summarized below. Let Φ_R be orthonormalized, i.e.

$$\Phi_R^T M \Phi_R = I \tag{21}$$

Define P as

$$P = I - M \Phi_R \Phi_R^T \tag{22}$$

Select a statically determinate subset from $\underline{x}_B$, denoted $\underline{x}_R$, and partition K as

$$K = \begin{bmatrix} K_{EE} & K_{ER} \\ K_{ER}^T & K_{RR} \end{bmatrix} \tag{23}$$

Now define a special flexibility matrix relative to the $\underline{x}_R$ DOF as

$$G^S = \begin{bmatrix} K_{EE}^{-1} & 0 \\ 0 & 0 \end{bmatrix} \tag{24}$$

Then it can be shown that

$$G^e = P^T G^S P \tag{25}$$

Then,

$$G^d = P^T G^S P - \Phi_{ke} \Omega_{ke}^{-2} \Phi_{ke}^T \tag{26}$$

is the required (N x N) residual flexibility matrix as given in Equation (5) which defines the inertia relief residual attachment modes.

NASTRAN DMAP Programming Considerations

The matrices given in Equations (18a,b) were DMAP programmed into rigid format Solution 63 in a very simple and straightforward manner. The eigenanalysis results from the READ module provided Φ_R and Φ_{ke} for each subsystem. P, G_I and G_B were then calculated using DMAP matrix operation modules. Finally, Equations (17a,b) were obtained to define the subsystem boundary level matrices, denoted KAAPRIME and MAAPRIME. The internally generated KLAA and MLAA matrices for each subsystem were purged from the data base and the superelement matrix assembly module (SEMA) was modified to

read KAAPRIME and MAAPRIME instead of the internally generated KAA and MAA matrices. The standard residual structure eigenanalysis in Solution 63 was then used to obtain the approximate system modes for the Method 3 calculations. This permitted results to be obtained for Method 3 using standard procedures in MSC/NASTRAN with minimal modification to the rigid format sequence.

The DMAP modifications required to calculate the MSCC's was slightly more involved. For all the CMS techniques, the full 318 length approximate eigenvector must first be reconstructed from its internally available representation, which exists only for each superelement individually. This is needed before the vector dot products in the MSCC equation can be calculated. In addition, for Method 3, a different transformation is required to obtain the $\underline{x}_O$ entries of the eigenvector. These may be calculated from the approximate eigenvector described by the $\underline{x}_B$ and $\underline{q}_k$ DOF using the upper partition of the total transformation

$$T_{tot} = T_1 T_2 \tag{27}$$

which, for the real eigenvalue problem simplifies to

$$\underline{x}_O = G_{OB} G_{BB}^{-1} \underline{x}_B + (\Phi_{kO} - G_{OB} G_{BB}^{-1} \Phi_{kB})\underline{q}_k \tag{28a}$$

$$= [\text{GOATPRIME}]\ \underline{x}_B + [\text{GOAQPRIME}]\ \underline{q}_k \tag{28b}$$

For each superelement, the two matrices defined in Equation (28b) were calculated to determine the static (physical coordinate) and dynamic (generalized coordinate) portions of the total transformation for the $\underline{x}_O$ DOF. The DMAP sequence was modified to retrieve the GOATPRIME and GOAQPRIME matrices instead of the internally generated GOAT and GOAQ

matrices for each subsystem to obtain the total GOA transformation for $\underline{x}_O$. The modified GOA transformation was then used to recover the dependent DOF for the eigenvectors, which are needed for the MSCC calculations and for plotting. GM, the standard internal transformation for recovering the multipoint constraint DOF (m-set), was not modified. Also, the standard plotting procedures in Solution 63 were used to obtain the mode shape plots.

Further work is needed to write a more user friendly DMAP program patterned after the general approach of rigid format Solution 41. This would use standard MSC/NASTRAN USET definitions to permit more useable definitions of the reduced subsystem and transformation matrices.